

A Hierarchical Bayesian Setting for an Inverse Problem in Linear Parabolic PDEs with Noisy Boundary Conditions

Fabrizio Ruggeri^{*}, Zaid Sawlan[†], Marco Scavino^{‡,§}, and Raul Tempone[¶]

Abstract. In this work we develop a Bayesian setting to infer unknown parameters in initial-boundary value problems related to linear parabolic partial differential equations. We realistically assume that the boundary data are noisy, for a given prescribed initial condition. We show how to derive the joint likelihood function for the forward problem, given some measurements of the solution field subject to Gaussian noise. Given Gaussian priors for the time-dependent Dirichlet boundary values, we analytically marginalize the joint likelihood using the linearity of the equation. Our hierarchical Bayesian approach is fully implemented in an example that involves the heat equation. In this example, the thermal diffusivity is the unknown parameter. We assume that the thermal diffusivity parameter can be modeled a priori through a lognormal random variable or by means of a space-dependent stationary lognormal random field. Synthetic data are used to test the inference. We exploit the behavior of the non-normalized log posterior distribution of the thermal diffusivity. Then, we use the Laplace method to obtain an approximated Gaussian posterior and therefore avoid costly Markov Chain Monte Carlo computations. Expected information gains and predictive posterior densities for observable quantities are numerically estimated using Laplace approximation for different experimental setups.

Keywords: linear parabolic PDEs, noisy boundary parameters, Bayesian inference, heat equation, thermal diffusivity.

1 Introduction

Parabolic partial differential equations model various important physical phenomena such as diffusion and heat transport. The solution of such equations propagates forward in time from an initial condition given boundary conditions and equation coefficients. In applications, some equation coefficients can be unknown quantities that need to be estimated. In addition, exact initial and boundary conditions might not be known.

^{*}CNR – IMATI, Consiglio Nazionale delle Ricerche, Milano, Italy, fabrizio@mi.imati.cnr.it

[†]Corresponding author. CEMSE, King Abdullah University of Science and Technology, Thuwal, 23955-6900, KSA, zaid.sawlan@kaust.edu.sa

[‡]CEMSE, King Abdullah University of Science and Technology, Thuwal, 23955-6900, KSA, marco.scavino@kaust.edu.sa

[§]Instituto de Estadística (IESTA), Universidad de la República, Montevideo, Uruguay, mscavino@iesta.edu.uy

[¶]CEMSE, King Abdullah University of Science and Technology, Thuwal, 23955-6900, KSA, raul.tempone@kaust.edu.sa

One possible approach to estimate these unknowns is to solve the inverse problem given some information about the solution. Classical inversion methods for parabolic partial differential equations are introduced by Samarskii and Vabishchevich (2007) in Chapter 8 of their book.

Several approaches on parameter estimation for PDE models are available in the literature. For example, Bär et al. (1999) have modeled the unknown PDEs as multivariate polynomials of the independent variables, then choose the best fit by computation of the nullclines of the fitted PDEs. Müller and Timmer (2002) have applied a two-stage generalization of the multiple shooting method to deal with the parameter estimation for nonlinear PDEs with noisy and partially observed data. A generalized smoothing approach for a system of nonlinear ordinary differential equations has been provided by Ramsay et al. (2007). Recently, Xun et al. (2013) have developed two methods to estimate parameters in PDE models: a parameter cascading method and a Bayesian method. In both approaches, the unknown dynamic process is represented by a linear combination of B-spline basis functions that, in the Bayesian approach, is estimated by the Bayesian P-spline method. Markov Chain Monte Carlo procedures have been used to sample from the posterior distributions of the PDE parameters and the B-spline coefficients. It is worth mentioning that most of such works address problems with nonlinear PDEs. These works do not exploit the linear structure for the efficient treatment of noisy initial and boundary conditions. Motivated by this fact, our goal in this work is to develop an efficient parameter estimation method that exploits the particular structure of linear time dependent PDEs. This extremely important class of PDEs includes, among others, the heat equation, the wave equation and the transport equation. Moreover, this class is broad enough to cover many crucial engineering applications and therefore deserves its own very efficient computational approach.

In this work, we consider a Bayesian inversion problem to determine the coefficients of linear parabolic partial differential equations, as an example of linear time dependent PDEs, under the assumption that noisy measurements are available in the interior of a domain of interest and for the unknown boundary conditions. A main novelty of our approach to solve the inverse problem relies on the assumption that the boundary parameters are unknown and modeled by means of adequate probability distributions. Subsequently, the contribution of the boundary parameters is marginalized out from the joint law with the unknown equation coefficients we want to infer, allowing the characterization of their posterior distribution. There are many advantages to a Bayesian approach. For example, it provides a solution along with a comprehensive measure of uncertainty given by the posterior distribution. Moreover, the prior available information can be easily incorporated in terms of elicited prior distributions (Ghosh et al., 2006). An important issue in this work is that Bayesian inversion is posed as a hierarchical process. Boundary conditions can therefore be treated as unknown parameters (Kaipio and Fox, 2011). Since we are only interested in estimating the equation coefficients, we eliminate those extra parameters by analytic marginalization. We show how to perform such analytical marginalization for a linear parabolic PDE in Section 4. This marginalization step allows us to compute the marginal likelihood very efficiently, yielding thus via numerical optimization posterior estimates of our unknown parameters, such as the maximum a posteriori estimate. We note in passing that for the case of nonlinear PDEs,

our analytic marginalization does not apply and more costly simulation-based schemes such as MCMC will be needed, as described in Xun et al. (2013).

Bayesian inversion techniques for the heat equation have been discussed and implemented in some previous works. Kaipio and Fox (2011) provided a general Bayesian framework for inverse problems in heat transfer, classified according to the dominant mode in heat transfer. The authors address many issues regarding forward problems and their statistical analysis. The prior modeling is extensively discussed, as well as how to deal, in particular, with different sources of uncertainties. Heat flux reconstruction problems have been studied by Wang and Zabarar (2005, 2004). When referring to the problem of parameter estimation in inverse heat conduction problems, Wang and Zabarar showed how to infer the thermal conductivity using a hierarchical Bayesian framework, on the basis of temperature readings within a conducting solid, assuming that the heat flux on the boundary and the heat source are known. They also explored the high dimensional posterior state space by means of Markov Chain Monte Carlo simulation. Lanzarone et al. (2014) estimated the thermal conductivity of a polymer, transforming the heat equation into a stochastic differential equation and considering the Euler–Maruyama approximation to get the likelihood, introducing latent observations in space and then using a relatively cumbersome Markov Chain Monte Carlo method. Fudym et al. (2008) and Massard et al. (2010) addressed the estimation problem of the thermal diffusivity, as in the present work, which is a parameter that describes thermophysical property of materials. In their works a large number of temperature measurements is made by an infrared camera, with fine spatial resolution and high frequency. They solved one and two-dimensional forward problems for transient heat conduction, with spatially varying thermal conductivity and volumetric heat capacity, by finite differences, according to a nodal strategy. The parameter vector at each node is then estimated either by minimizing an a posteriori objective function when prior Gaussian distributions are assumed for the parameters, or by means of Markov Chain Monte Carlo methods for different prior distributions.

This work is organized as follows. In Section 2, we introduce the statistical setting and we derive the explicit form of the joint law of the unknown equation coefficients and the boundary parameters. In Section 3, we use a finite element scheme in order to write the solution of the forward problem as a linear function of the boundary conditions. We demonstrate in Section 4 that, under certain conditions, an exact marginalization can be carried out, yielding a closed formula for the marginal likelihood of the equation coefficients. In Section 5, we apply our marginalization technique to estimating thermal diffusivity in the one-dimensional heat equation in two cases given temperature simulated data. Numerical results are obtained for the non-normalized log posterior distribution of the thermal diffusivity. We model prior knowledge about the thermal diffusivity first as a lognormal random variable and then using a lognormal random field with a squared exponential (SE) covariance function (Rasmussen and Williams, 2006). In the first case, we use the Laplace method to provide an approximated Gaussian posterior distribution for the thermal diffusivity. Such method is then applied to obtain fast estimations of the information gain and the expected information gain under three experimental setups, and the predictive posterior mean of the temperature is also derived using the inferred thermal diffusivity. In the second case, where the thermal

diffusivity is allowed to depend on the spatial variable, the Laplace approximation is used to obtain the posterior distribution of the hyperparameters that characterize the prior distribution for the thermal diffusivity.

2 Statistical setting and preliminary results

In this section we introduce the statistical model associated to the forward initial-boundary value problems for linear parabolic partial differential equations. We then derive, under mild assumptions, the exact expression for the joint likelihood function of the unknown parameters in the parabolic equation and the unknown boundary parameters.

Consider the deterministic one-dimensional parabolic initial-boundary value problem:

$$\begin{cases} \partial_t T + L_{\theta} T = 0, & x \in (x_L, x_R), 0 < t \leq t_N < \infty \\ T(x_L, t) = T_L(t), & t \in [0, t_N] \\ T(x_R, t) = T_R(t), & t \in [0, t_N] \\ T(x, 0) = g(x), & x \in (x_L, x_R), \end{cases} \quad (1)$$

where L_{θ} is a linear second-order partial differential operator that takes the form

$$L_{\theta} T = -\partial_x(a(x)\partial_x T) + b(x)\partial_x T + c(x)T,$$

$\theta(x) = (a(x), b(x), c(x))^{tr}$, and the partial differential operator $\partial_t + L_{\theta}$ is parabolic, because (Evans (1998), p. 372) there exists ϵ such that $a(x) \geq \epsilon > 0$ for all $x \in (x_L, x_R)$. We also assume that

- P1 a, b and c are bounded functions.
- P2 T_L, T_R and g are square integrable functions.
- P3 The initial condition, g , is consistent with the boundary functions, namely $g(x_L) = T_L(0)$ and $g(x_R) = T_R(0)$.

Then, under the assumptions P1–P3, there exists a unique weak solution of (1) (Evans (1998), pp. 375–377).

Our main objective is to provide a Bayesian solution to an inverse problem for θ , where we assume that

- i θ is unknown, while the initial condition g in the initial-boundary value problem is known;
- ii θ is allowed to vary with the spatial variable x .

Remark 1. *In our Bayesian approach, we will assume later that the coefficient $a(x)$ is a lognormal random variable or lognormal random field. Therefore, $a(x)$ will not be*

bounded as assumed in P1. However, it can be proved that there exists a unique solution of the stochastic parabolic initial-boundary value problem in the space $L^2(\Omega, H^1)$. Such proof can be found in Charrier (2012) for elliptic boundary value problems but it can be also extended to parabolic initial-boundary value problems.

Given noisy readings of the function $T(x, t)$ at the $I + 1$ spatial locations, including the boundaries, $x_L = x_0, x_1, x_2, \dots, x_{I-1}, x_I = x_R$, at each of the N times t_1, t_2, \dots, t_N , we want to infer θ using a Bayesian approach. To determine the posterior distribution for θ , we need first to obtain the likelihood function of θ . The remainder of this section derives the joint likelihood function of θ and the boundary parameters. Let us introduce some convenient notation and assumptions: let $\mathbf{Y}_n := (Y_{0,n}, \dots, Y_{I,n})^{tr}$ denote the vector of observed readings at time t_n , and assume a statistical model with an additive Gaussian experimental noise ϵ_n ; that is:

$$\mathbf{Y}_n \stackrel{(I+1) \times 1}{=} \begin{bmatrix} T_L(t_n) \\ T(x_1, t_n) \\ \vdots \\ T(x_{I-1}, t_n) \\ T_R(t_n) \end{bmatrix} + \epsilon_n, \tag{2}$$

where $\epsilon_n \stackrel{\text{i.i.d.}}{\sim} \mathcal{N}(\mathbf{0}_{I+1}, \sigma^2 \mathbf{I}_{I+1})$ for some measurement error variance $\sigma^2 > 0$. The covariance matrix of ϵ_n is assumed equal to $\sigma^2 \mathbf{I}_{I+1}$ for simplicity, a general covariance matrix Σ_{ϵ_n} could be used as well provided that the boundary measurement errors are independent from the interior measurement errors. Also denote by $\mathbf{Y}_n^I := (Y_{1,n}, \dots, Y_{I-1,n})^{tr}$ the vector of observed data at the interior locations x_1, x_2, \dots, x_{I-1} and let $\mathbf{Y}_n^B := (Y_{L,n}, Y_{R,n})^{tr}$ be the vector of observed data at the boundary locations x_0, x_I at time t_n . The density of \mathbf{Y}_n^I is derived as it follows. First consider the time local problem, defined between consecutive measurement times, i.e.

$$\begin{cases} \partial_t T + L_\theta T = 0, & x \in (x_L, x_R), t_{n-1} < t \leq t_n, \\ T(x_L, t) = T_L(t), & t \in [t_{n-1}, t_n], \\ T(x_R, t) = T_R(t), & t \in [t_{n-1}, t_n], \\ T(x, t_{n-1}) = \widehat{T}(x, t_{n-1}), & x \in (x_L, x_R), \end{cases} \tag{3}$$

whose exact solution, denoted by $\widehat{T}(\cdot, t_n)$, depends only on $\theta, \widehat{T}(\cdot, t_{n-1})$ and the boundary values $\{T_L(t), T_R(t)\}_{t \in (t_{n-1}, t_n)}$. Finally, use the form of the statistical model (2) to obtain the form of the density of \mathbf{Y}_n^I .

Lemma 2. *Given the model (2), the probability density function of \mathbf{Y}_n^I is expressed as*

$$\rho(\mathbf{Y}_n^I | \theta, \widehat{T}(\cdot, t_{n-1}), \{T_L(t), T_R(t)\}_{t \in (t_{n-1}, t_n)}) = \frac{1}{(\sqrt{2\pi}\sigma)^{I-1}} \exp\left(-\frac{1}{2\sigma^2} \|\mathbf{R}_{t_n}\|_{\ell^2}^2\right), \tag{4}$$

where $\mathbf{R}_{t_n} \stackrel{(I-1) \times 1}{:=} (\widehat{T}(x_1, t_n) - Y_{1,n}, \dots, \widehat{T}(x_{I-1}, t_n) - Y_{I-1,n})^{tr}$ denotes the data residual vector at time $t = t_n$.

For illustration purposes and without loss of generality, assume now that the Dirichlet boundary condition functions, $T_L(\cdot)$ and $T_R(\cdot)$, are well approximated by piecewise linear continuous functions in the time partition $\{t_n\}_{n=1,\dots,N}$.

In this way, only $2N$ parameters, say $T_L(t_n) = T_{L,n}$, $T_R(t_n) = T_{R,n}$, $n = 1, 2, \dots, N$, suffice to determine the boundary conditions that are, in principle, infinite dimensional parameters. Let LBC_n denote the time nodes that determine the local boundary conditions $\{T_{L,n-1}, T_{L,n}, T_{R,n-1}, T_{R,n}\}$. Other interpolation schemes may be used as well.

Remark 3. Given the discretized Dirichlet boundary conditions introduced above, we can say that $\widehat{T}(\cdot, t_n)$ depends only on $\boldsymbol{\theta}, T(\cdot, t_{n-1})$ and the boundary parameters LBC_n . Similarly, $\widehat{T}(\cdot, t_{n-1})$ depends on $\boldsymbol{\theta}, T(\cdot, t_{n-2})$ and the boundary parameters LBC_{n-1} . From this recursion, we can obtain

$$\rho(\mathbf{Y}_n^I | \boldsymbol{\theta}, g, \{LBC_j\}_{j=1,\dots,n}) = \rho(\mathbf{Y}_n^I | \boldsymbol{\theta}, \widehat{T}(\cdot, t_{n-1}), LBC_n). \quad (5)$$

Since the initial condition, g , is assumed to be known, it will be omitted in the rest of the paper.

Lemma 4. Given the model (2) and Lemma 2, the joint likelihood function of $\boldsymbol{\theta}$ and the boundary parameters $\{LBC_n\}_{n=1,\dots,N}$ is given by

$$\begin{aligned} \rho(\mathbf{Y}_1, \dots, \mathbf{Y}_N | \boldsymbol{\theta}, \{LBC_n\}_{n=1,\dots,N}) &= \prod_{n=1}^N \frac{1}{(\sqrt{2\pi}\sigma)^{I-1}} \exp\left(-\frac{1}{2\sigma^2} \|\mathbf{R}_{t_n}\|_{\ell^2}^2\right) \\ &\times \frac{1}{\sqrt{2\pi\sigma^2}} \exp\left(-\frac{1}{2\sigma^2} (T_{L,n} - Y_{L,n})^2\right) \frac{1}{\sqrt{2\pi\sigma^2}} \exp\left(-\frac{1}{2\sigma^2} (T_{R,n} - Y_{R,n})^2\right). \quad (6) \end{aligned}$$

Proof. Observe that $\mathbf{Y}_n^I, \mathbf{Y}_n^B$ are conditionally independent given $\boldsymbol{\theta}, \widehat{T}(\cdot, t_{n-1}), LBC_n$. Thus, we have

$$\begin{aligned} \rho(\mathbf{Y}_n | \boldsymbol{\theta}, \widehat{T}(\cdot, t_{n-1}), LBC_n) &= \rho(\mathbf{Y}_n^I, \mathbf{Y}_n^B | \boldsymbol{\theta}, \widehat{T}(\cdot, t_{n-1}), LBC_n), \\ &= \rho(\mathbf{Y}_n^I | \boldsymbol{\theta}, \widehat{T}(\cdot, t_{n-1}), LBC_n) \times \rho(\mathbf{Y}_n^B | \boldsymbol{\theta}, \widehat{T}(\cdot, t_{n-1}), LBC_n), \\ &= \rho(\mathbf{Y}_n^I | \boldsymbol{\theta}, \widehat{T}(\cdot, t_{n-1}), LBC_n) \times \rho(\mathbf{Y}_n^B | LBC_n) \end{aligned}$$

since $\mathbf{Y}_n^B | LBC_n$ does not depend on either $\boldsymbol{\theta}$ nor $\widehat{T}(\cdot, t_{n-1})$.

The joint likelihood function can then be written as

$$\begin{aligned} &\rho(\mathbf{Y}_1, \dots, \mathbf{Y}_N | \boldsymbol{\theta}, \{LBC_n\}_{n=1,\dots,N}) \\ &= \rho(\mathbf{Y}_N | \boldsymbol{\theta}, \{LBC_n\}_{n=1,\dots,N}, \mathbf{Y}_{N-1}, \dots, \mathbf{Y}_1) \times \rho(\mathbf{Y}_1, \dots, \mathbf{Y}_{N-1} | \boldsymbol{\theta}, \{LBC_n\}_{n=1,\dots,N-1}) \\ &(\text{since } \mathbf{Y}_N | \boldsymbol{\theta}, \{LBC_n\}_{n=1,\dots,N} \text{ is independent from } \mathbf{Y}_1, \dots, \mathbf{Y}_{N-1}) \\ &= \rho(\mathbf{Y}_N | \boldsymbol{\theta}, \{LBC_n\}_{n=1,\dots,N}) \times \rho(\mathbf{Y}_1, \dots, \mathbf{Y}_{N-1} | \boldsymbol{\theta}, \{LBC_n\}_{n=1,\dots,N-1}) \\ &(\text{using equation (5)}) \\ &= \rho(\mathbf{Y}_N | \boldsymbol{\theta}, \widehat{T}(\cdot, t_{N-1}), LBC_N) \times \rho(\mathbf{Y}_1, \dots, \mathbf{Y}_{N-1} | \boldsymbol{\theta}, \{LBC_n\}_{n=1,\dots,N-1}) \end{aligned}$$

(iterating the previous arguments)

$$= \prod_{n=1}^N \rho(\mathbf{Y}_n | \boldsymbol{\theta}, \widehat{T}(\cdot, t_{n-1}), LBC_n) = \prod_{n=1}^N \rho(\mathbf{Y}_n^I | \boldsymbol{\theta}, \widehat{T}(\cdot, t_{n-1}), LBC_n) \times \rho(\mathbf{Y}_n^B | LBC_n)$$

and finally, using (4), the expression (6) is obtained. \square

Remark 5. A generalization of the joint likelihood can be obtained given serial correlations, that is, $\{\boldsymbol{\epsilon}_n\}_{n=1}^N$ are time correlated.

Using the notation $\mathbf{T}_L = (T_{L,1}, \dots, T_{L,N})^{tr}$, $\mathbf{T}_R = (T_{R,1}, \dots, T_{R,N})^{tr}$, $\mathbf{Y}_L = (Y_{L,1}, \dots, Y_{L,N})^{tr}$ and $\mathbf{Y}_R = (Y_{R,1}, \dots, Y_{R,N})^{tr}$, the joint likelihood function (6) can be written as

$$\begin{aligned} \rho(\mathbf{Y}_1, \dots, \mathbf{Y}_N | \boldsymbol{\theta}, \mathbf{T}_L, \mathbf{T}_R) &= (\sqrt{2\pi}\sigma)^{-N(I+1)} \exp\left(-\frac{1}{2\sigma^2} \sum_{n=1}^N \|\mathbf{R}_{t_n}\|_{\ell^2}^2\right) \\ &\times \exp\left(-\frac{1}{2\sigma^2} \left[\|\mathbf{T}_L - \mathbf{Y}_L\|_{\ell^2}^2 + \|\mathbf{T}_R - \mathbf{Y}_R\|_{\ell^2}^2\right]\right), \end{aligned} \quad (7)$$

which is a suitable expression to derive later the marginal likelihood of $\boldsymbol{\theta}$. The prior distributions for $\boldsymbol{\theta}$ and the boundary parameters $\mathbf{T}_L, \mathbf{T}_R$ can be specified in different ways. Generally speaking, the prior distribution for $\boldsymbol{\theta}$ should be proposed according to the physical properties described by the unknown parameters and taking into account available prior knowledge about the observed phenomena. As an example, it is known that the thermal conductivity of polymethyl methacrylate (plexiglas) is in the range 0.167–0.25 W/(mK). A uniform prior distribution for the thermal conductivity could be chosen if there is no preference among the values of the interval.

As per the boundary parameters, we assume independent Gaussian models $T_{L,n} \sim \mathcal{N}(\mu_{L,n}, \sigma_p^2)$, $T_{R,n} \sim \mathcal{N}(\mu_{R,n}, \sigma_p^2)$, $n = 1, \dots, N$, with means $\boldsymbol{\mu}_L = (\mu_{L,1}, \dots, \mu_{L,N})^{tr}$, $\boldsymbol{\mu}_R = (\mu_{R,1}, \dots, \mu_{R,N})^{tr}$, and variance $\sigma_p^2 > 0$. The mean vectors $\boldsymbol{\mu}_L$ and $\boldsymbol{\mu}_R$ can be either known beforehand or constructed from a subsample of the boundary data \mathbf{Y}_L and \mathbf{Y}_R . In the latter case, the likelihood function (7) should be modified accordingly. For simplicity, hereafter we assume that $\boldsymbol{\mu}_L$ and $\boldsymbol{\mu}_R$ are known beforehand.

We claim that the data residual vector \mathbf{R}_{t_n} can be written as a linear function of \mathbf{T}_L and \mathbf{T}_R . The next section is devoted to the proof of this basic result. This proof allows for the exact marginalization of the contribution of the nuisance boundary parameters from the joint likelihood function (7).

3 Numerical approximation

In this section, our goal is to approximate the residual vector \mathbf{R}_{t_n} as a linear function of the boundary conditions. After reformulating the main problem (1), as described in the next lemma, we will introduce its weak form and finite element method will be then applied to provide a numerical approximation of the solution of the weak problem.

Lemma 6. *The solution of (1) can be written in the form*

$$T(x, t) = T_L(t) \frac{x_R - x}{x_R - x_L} + T_R(t) \frac{x - x_L}{x_R - x_L} + u(x, t), \quad (8)$$

where u solves a new initial-boundary value problem with homogeneous Dirichlet boundary conditions:

$$\begin{cases} \partial_t u + L_{\theta} u = f(x, t), & x \in (x_L, x_R), 0 < t \leq t_N < \infty \\ u(x_L, t) = 0, & t \in [0, t_N] \\ u(x_R, t) = 0, & t \in [0, t_N] \\ u(x, 0) = g^0(x), & x \in (x_L, x_R) \end{cases} \quad (9)$$

and

$$\begin{aligned} f(x, t) &= -(\partial_t + L_{\theta}) T_L(t) \frac{x_R - x}{x_R - x_L} - (\partial_t + L_{\theta}) T_R(t) \frac{x - x_L}{x_R - x_L}, \\ g^0(x) &= g(x) - T_L(0) \frac{x_R - x}{x_R - x_L} - T_R(0) \frac{x - x_L}{x_R - x_L}. \end{aligned}$$

We now introduce the weak formulation of problem (9).

Find $u(t) \in V = H_0^1(x_L, x_R)$, $t \in (0, t_N)$ such that:

$$\begin{cases} \int_{x_L}^{x_R} \partial_t u(t) v dx + B(u(t), v) = \int_{x_L}^{x_R} f(t) v dx, \forall v \in V, t \in (0, t_N), \\ u(0) = g^0, x \in (x_L, x_R), \end{cases} \quad (10)$$

where $B(u, v) = \int_{x_L}^{x_R} [a(x) \partial_x u \partial_x v + b(x) \partial_x u v + c(x) u v] dx$ and $H_0^1(x_L, x_R)$ is the closure of the space $C_c^1(x_L, x_R)$ of continuously differentiable functions with compact support on (x_L, x_R) with respect to the H^1 -norm (Johnson (1987), p. 149).

Given a mesh $x_L = x_0 < \dots < k\Delta x = x_k < \dots < I\Delta x = x_I = x_R$ of the spatial domain (x_L, x_R) , we apply the finite element method with piecewise linear functions (hat functions) $\{\phi_k\}_{k=1}^{I-1}$ to approximate the weak solution $u(x, t)$ of (9) as linear combinations of the basis functions:

$$u(x, t) \approx u_{\Delta x}(x, t) = \sum_{k=1}^{I-1} u_k(t) \phi_k(x), \quad 0 < t \leq t_N,$$

and we get

$$\sum_{k=1}^{I-1} \partial_t u_k(t) \int_{x_L}^{x_R} \phi_k \phi_j dx + \sum_{k=1}^{I-1} u_k(t) B(\phi_k, \phi_j) = \int_{x_L}^{x_R} f(t) \phi_j dx, \quad j = 1, \dots, I-1, t \in (0, t_N). \quad (11)$$

Let $\mathbf{u}(t) = (u_1(t), \dots, u_{I-1}(t))^{tr}$, then we can write the linear system of ODEs (11) in a matrix form as:

$$M \partial_t \mathbf{u}(t) + S_{\theta} \mathbf{u}(t) = \mathbf{f}(t), \quad 0 < t \leq t_N, \quad (12)$$

where M is the mass matrix, S_{θ} is the stiffness matrix and $\mathbf{f}(t)$ is the load vector.

We consider now a uniform time discretization of $(0, t_N)$ such that $t_0 = 0 < \dots < n\Delta t = t_n < \dots < N\Delta t = t_N$ and denote $\mathbf{u}(t_n) = \mathbf{u}_n$ and $\mathbf{f}(t_n) = \mathbf{f}_n$. We apply the backward Euler method on equation (12) to obtain the fully discrete analogue of (10) that takes the form

$$\begin{cases} (M + \Delta t S_{\theta}) \mathbf{u}_{n+1} = M \mathbf{u}_n + \Delta t \mathbf{f}_{n+1}, n = 0, \dots, N-1, \\ M \mathbf{u}_0 = \mathbf{g}^0, \end{cases} \quad (13)$$

where $\mathbf{g}^0 = (\int_{x_L}^{x_R} g^0 \phi_1 dx, \dots, \int_{x_L}^{x_R} g^0 \phi_{I-1} dx)^{tr}$.

Theorem 7. *The approximation of the weak solution of (9) can be written as a linear function of the initial and boundary conditions:*

$$\mathbf{u}_n = A_n(\theta) \mathbf{u}_0 + \tilde{A}_{L,n}(\theta) \mathbf{T}_L + \tilde{A}_{R,n}(\theta) \mathbf{T}_R, \quad (14)$$

where $\mathbf{u}_n = (u_{1,n}, \dots, u_{I-1,n})^{tr}$, $\mathbf{T}_L = (T_{L,1}, \dots, T_{L,N})^{tr}$, $\mathbf{T}_R = (T_{R,1}, \dots, T_{R,N})^{tr}$, and the matrices $A_n(\theta)$, $\tilde{A}_{L,n}(\theta)$ and $\tilde{A}_{R,n}(\theta)$ are explicitly constructed in the proof.

Proof. See Appendix A of the Supplementary Material (Ruggeri et al., 2016). \square

Theorem 8. *The approximation of the weak solution of (1) can be written as a linear function of the initial and boundary conditions:*

$$\mathbf{T}_n = \mathbf{B}^n \mathbf{T}_0 + A_{L,n}(\theta) \mathbf{T}_L + A_{R,n}(\theta) \mathbf{T}_R. \quad (15)$$

where \mathbf{T}_n is defined similarly to \mathbf{u}_n and the matrices \mathbf{B} , $A_{L,n}(\theta)$ and $A_{R,n}(\theta)$ are explicitly constructed in the proof.

Proof. See Appendix B of the Supplementary Material. \square

Remark 9. *The weak solution of two-dimensional and higher dimensional linear parabolic PDEs can be written in a similar form of equation (15) (see Johnson (1987), pp. 149–156).*

Corollary 10. *The data residual vector $\mathbf{R}_{t_n} = (\hat{T}(x_1, t_n) - Y_{1,n}, \dots, \hat{T}(x_{I-1}, t_n) - Y_{I-1,n})^{tr}$ is approximated by*

$$\tilde{\mathbf{R}}_{t_n} = (\mathbf{B}^n \mathbf{T}_0 - \mathbf{Y}_n^I) + A_{L,n}(\theta) \mathbf{T}_L + A_{R,n}(\theta) \mathbf{T}_R. \quad (16)$$

4 The marginal likelihood of θ

Given the observations $\mathbf{Y}_1, \dots, \mathbf{Y}_N$, we showed, in Section 2, how to obtain the joint likelihood function of θ and the boundary parameters $\mathbf{T}_L, \mathbf{T}_R$.

In the present section, we derive a convenient expression for the marginal likelihood of θ , under the assumption that the prior distributions for \mathbf{T}_L and \mathbf{T}_R are independent Gaussian:

$$\mathbf{T}_L \sim \mathcal{N}(\boldsymbol{\mu}_L, \sigma_p^2 \mathbf{I}_N), \quad \mathbf{T}_R \sim \mathcal{N}(\boldsymbol{\mu}_R, \sigma_p^2 \mathbf{I}_N), \quad (17)$$

Then, using (7), the marginal likelihood of $\boldsymbol{\theta}$ is given by:

$$\begin{aligned}
\rho(\mathbf{Y}_1, \dots, \mathbf{Y}_N | \boldsymbol{\theta}) &= (\sqrt{2\pi}\sigma)^{-N(I+1)} \times (\sqrt{2\pi}\sigma_p)^{-2N} \int_{\mathcal{T}_R} \int_{\mathcal{T}_L} \exp\left(-\frac{1}{2\sigma^2} \sum_{n=1}^N \|\mathbf{R}_{t_n}\|_{\ell^2}^2\right) \\
&\quad \times \exp\left(-\frac{1}{2\sigma^2} (\mathbf{T}_L - \mathbf{Y}_L)^{tr} (\mathbf{T}_L - \mathbf{Y}_L) \right. \\
&\quad \left. - \frac{1}{2\sigma^2} (\mathbf{T}_R - \mathbf{Y}_R)^{tr} (\mathbf{T}_R - \mathbf{Y}_R)\right) \\
&\quad \times \exp\left(-\frac{1}{2\sigma_p^2} (\mathbf{T}_L - \boldsymbol{\mu}_L)^{tr} (\mathbf{T}_L - \boldsymbol{\mu}_L) \right. \\
&\quad \left. - \frac{1}{2\sigma_p^2} (\mathbf{T}_R - \boldsymbol{\mu}_R)^{tr} (\mathbf{T}_R - \boldsymbol{\mu}_R)\right) d\mathbf{T}_L d\mathbf{T}_R. \tag{18}
\end{aligned}$$

To provide the exact expression of the marginal likelihood of the linear parabolic equation coefficients $\boldsymbol{\theta}$, which has been implemented in the computational examples presented in Section 5, it is convenient to introduce the following notation:

$$\begin{aligned}
\Delta_{L,N} &= \sum_{n=1}^N A_{L,n}(\boldsymbol{\theta})^{tr} A_{L,n}(\boldsymbol{\theta}), \quad \Delta_{R,N} = \sum_{n=1}^N A_{R,n}(\boldsymbol{\theta})^{tr} A_{R,n}(\boldsymbol{\theta}), \\
\Delta_{2,L,N} &= \sum_{n=1}^N A_{L,n}(\boldsymbol{\theta})^{tr} (\mathbf{Y}_n^I - \mathbf{B}^n \mathbf{T}_0), \quad \Delta_{2,R,N} = \sum_{n=1}^N A_{R,n}(\boldsymbol{\theta})^{tr} (\mathbf{Y}_n^I - \mathbf{B}^n \mathbf{T}_0), \\
A_{L,R,N} &= \sum_{n=1}^N A_{L,n}(\boldsymbol{\theta})^{tr} A_{R,n}(\boldsymbol{\theta}), \quad D_{\sigma^2} = \frac{1}{\sigma^2} \mathbf{I}_N, \quad D_{\sigma_p^2} = \frac{1}{\sigma_p^2} \mathbf{I}_N.
\end{aligned}$$

Theorem 11. *The marginal likelihood of $\boldsymbol{\theta}$ is given by:*

$$\begin{aligned}
\rho(\mathbf{Y}_1, \dots, \mathbf{Y}_N | \boldsymbol{\theta}) &= (\sqrt{2\pi}\sigma)^{-N(I+1)} (\sqrt{2\pi}\sigma_p)^{-2N} (2\pi)^{N/2} |\Lambda_0|^{1/2} (2\pi)^{N/2} |\Lambda_1|^{1/2} \\
&\quad \times \exp\left\{-\frac{1}{2\sigma^2} \left[\mathbf{Y}_L^{tr} \mathbf{Y}_L + \mathbf{Y}_R^{tr} \mathbf{Y}_R \right. \right. \\
&\quad \left. \left. + \sum_{i=1}^N (\mathbf{Y}_n^I - \mathbf{B}^n \mathbf{T}_0)^{tr} (\mathbf{Y}_n^I - \mathbf{B}^n \mathbf{T}_0) \right] - \frac{1}{2\sigma_p^2} [\boldsymbol{\mu}_L^{tr} \boldsymbol{\mu}_L + \boldsymbol{\mu}_R^{tr} \boldsymbol{\mu}_R] \right. \\
&\quad \left. + \frac{1}{2} (\boldsymbol{\mu}_L^{tr} D_{\sigma_p^2} + \mathbf{Y}_L^{tr} D_{\sigma^2} + \Delta_{2,L}^{tr} D_{\sigma^2}) \right. \\
&\quad \left. \times \Lambda_0 (D_{\sigma_p^2} \boldsymbol{\mu}_L + D_{\sigma^2} \mathbf{Y}_L + D_{\sigma^2} \Delta_{2,L}) \right. \\
&\quad \left. + \frac{1}{2} [\mathbf{t}_{R,2}^{tr} \Lambda_1 \mathbf{t}_{R,2} + 2\mathbf{t}_{R,3}^{tr} \Lambda_1 \mathbf{t}_{R,2} + \mathbf{t}_{R,3}^{tr} \Lambda_1 \mathbf{t}_{R,3}] \right\}, \tag{19}
\end{aligned}$$

where $\Lambda_0, \Lambda_1, \mathbf{t}_{R,2}$ and $\mathbf{t}_{R,3}$ are independent of \mathbf{T}_L and \mathbf{T}_R .

Proof. First, we observe that (18) can be written as:

$$\begin{aligned}
& (\sqrt{2\pi}\sigma)^{-N(I+1)} \times (\sqrt{2\pi}\sigma_p)^{-2N} \times \exp \left\{ -\frac{1}{2\sigma_p^2} [\boldsymbol{\mu}_L^{tr} \boldsymbol{\mu}_L + \boldsymbol{\mu}_R^{tr} \boldsymbol{\mu}_R] \right. \\
& \left. - \frac{1}{2\sigma^2} \left[\mathbf{Y}_L^{tr} \mathbf{Y}_L + \mathbf{Y}_R^{tr} \mathbf{Y}_R + \sum_{n=1}^N (\mathbf{Y}_n^I - \mathbf{B}^n \mathbf{T}_0)^{tr} (\mathbf{Y}_n^I - \mathbf{B}^n \mathbf{T}_0) \right] \right\} \\
& \times \int_{\mathcal{T}_R} \int_{\mathcal{T}_L} \exp \left\{ -\frac{1}{2} \left[\mathbf{T}_L^{tr} (D_{\sigma^2} + D_{\sigma_p^2} + \frac{1}{\sigma^2} \Delta_L) \mathbf{T}_L \right. \right. \\
& - 2(\boldsymbol{\mu}_L^{tr} D_{\sigma_p^2} + \mathbf{Y}_L^{tr} D_{\sigma^2} + \Delta_{2,L}^{tr} D_{\sigma^2}) \mathbf{T}_L + \frac{2}{\sigma^2} \mathbf{T}_R^{tr} A_{LR}^{tr} \mathbf{T}_L \\
& \left. \left. + \mathbf{T}_R^{tr} (D_{\sigma^2} + D_{\sigma_p^2} + \frac{1}{\sigma^2} \Delta_R) \mathbf{T}_R - 2(\boldsymbol{\mu}_R^{tr} D_{\sigma_p^2} + \mathbf{Y}_R^{tr} D_{\sigma^2} + \Delta_{2,R}^{tr} D_{\sigma^2}) \mathbf{T}_R \right] \right\} d\mathbf{T}_L d\mathbf{T}_R.
\end{aligned}$$

To marginalize \mathbf{T}_L and \mathbf{T}_R , we assume that they are independent Gaussian random vectors. We can then use the following standard result: if $\mathbf{X} \sim \mathcal{N}_p(\boldsymbol{\mu}, \boldsymbol{\Sigma})$, then $E(\exp(\mathbf{t}^{tr} \mathbf{X})) = \exp(\mathbf{t}^{tr} \boldsymbol{\mu} + \frac{1}{2} \mathbf{t}^{tr} \boldsymbol{\Sigma} \mathbf{t})$.

Therefore, by integrating first with respect to \mathbf{T}_L , the marginal likelihood of $\boldsymbol{\theta}$ and \mathbf{T}_R is proportional to the product of a factor that is independent of \mathbf{T}_L and the following term

$$\int_{\mathcal{T}_L} \exp \left\{ -\frac{1}{2} \mathbf{T}_L^{tr} \left(D_{\sigma^2} + D_{\sigma_p^2} + \frac{1}{\sigma^2} \Delta_L \right) \mathbf{T}_L \right\} \exp(\mathbf{t}_{L,1}^{tr} \mathbf{T}_L) d\mathbf{T}_L,$$

where

$$\mathbf{t}_{L,1}^{tr} = (\boldsymbol{\mu}_L^{tr} D_{\sigma_p^2} + \mathbf{Y}_L^{tr} D_{\sigma^2} + \Delta_{2,L}^{tr} D_{\sigma^2}) - \frac{1}{\sigma^2} \mathbf{T}_R^{tr} A_{LR}^{tr}.$$

It is now convenient to define $\Lambda_0^{-1} := (D_{\sigma^2} + D_{\sigma_p^2} + \frac{1}{\sigma^2} \Delta_L)$. The marginal likelihood of $\boldsymbol{\theta}$ and \mathbf{T}_R is proportional to the product of a factor that is independent of \mathbf{T}_L and the term $(2\pi)^{N/2} |\Lambda_0|^{1/2} \exp\{\frac{1}{2} \mathbf{t}_{L,1}^{tr} \Lambda_0 \mathbf{t}_{L,1}\}$.

Therefore, the marginal likelihood of $\boldsymbol{\theta}$ can be explicitly written as

$$\begin{aligned}
& (\sqrt{2\pi}\sigma)^{-N(I+1)} \times (\sqrt{2\pi}\sigma_p)^{-2N} \times (2\pi)^{N/2} |\Lambda_0|^{1/2} \times \exp \left\{ -\frac{1}{2\sigma_p^2} (\boldsymbol{\mu}_L^{tr} \boldsymbol{\mu}_L + \boldsymbol{\mu}_R^{tr} \boldsymbol{\mu}_R) \right. \\
& \left. - \frac{1}{2\sigma^2} \left[\mathbf{Y}_L^{tr} \mathbf{Y}_L + \mathbf{Y}_R^{tr} \mathbf{Y}_R + \sum_{i=1}^N (\mathbf{Y}_n^I - \mathbf{B}^n \mathbf{T}_0)^{tr} (\mathbf{Y}_n^I - \mathbf{B}^n \mathbf{T}_0) \right] \right\} \times \int_{\mathcal{T}_R} \exp \left\{ \frac{1}{2} \mathbf{t}_{L,1}^{tr} \Lambda_0 \mathbf{t}_{L,1} \right. \\
& \left. - \frac{1}{2} \left[\mathbf{T}_R^{tr} (D_{\sigma^2} + D_{\sigma_p^2} + \frac{1}{\sigma^2} \Delta_R) \mathbf{T}_R - 2(\boldsymbol{\mu}_R^{tr} D_{\sigma_p^2} + \mathbf{Y}_R^{tr} D_{\sigma^2} + \Delta_{2,R}^{tr} D_{\sigma^2}) \mathbf{T}_R \right] \right\} d\mathbf{T}_R.
\end{aligned}$$

The entire last expression is equal to the product of a term that is independent of \mathbf{T}_R and the following term:

$$\int_{\mathcal{T}_R} \exp \left\{ -\frac{1}{2} \mathbf{T}_R^{tr} \left[(D_{\sigma^2} + D_{\sigma_p^2} + \frac{1}{\sigma^2} \Delta_R) - \left(\frac{1}{\sigma^2} \right)^2 A_{LR}^{tr} \Lambda_0 A_{LR} \right] \mathbf{T}_R \right\} \times \exp \{ \mathbf{t}_{R,1}^{tr} \mathbf{T}_R \} d\mathbf{T}_R,$$

where

$$\mathbf{t}_{R,1}^{tr} = \underbrace{(\boldsymbol{\mu}_R^{tr} D_{\sigma_p^2} + \mathbf{Y}_R^{tr} D_{\sigma^2} + \Delta_{2,R}^{tr} D_{\sigma^2})}_{\mathbf{t}_{R,2}^{tr}} - \underbrace{(\boldsymbol{\mu}_L^{tr} D_{\sigma_p^2} + \mathbf{Y}_L^{tr} D_{\sigma^2} + \Delta_{2,L}^{tr} D_{\sigma^2})}_{\mathbf{t}_{R,3}^{tr}} \Lambda_0 A_{LR}.$$

If we now define $\Lambda_1^{-1} := (D_{\sigma^2} + D_{\sigma_p^2} + \frac{1}{\sigma^2} \Delta_R) - (\frac{1}{\sigma^2})^2 A_{LR}^{tr} \Lambda_0 A_{LR}$ and integrate with respect to \mathbf{T}_R , we have

$$\begin{aligned} \int_{\mathcal{T}_R} \exp \left\{ -\frac{1}{2} \mathbf{T}_R^{tr} \Lambda_1^{-1} \mathbf{T}_R \right\} \exp(\mathbf{t}_{R,1}^{tr} \mathbf{T}_R) d\mathbf{T}_R &= (2\pi)^{N/2} |\Lambda_1|^{1/2} \exp \left\{ \frac{1}{2} \mathbf{t}_{R,1}^{tr} \Lambda_1 \mathbf{t}_{R,1} \right\} \\ &= (2\pi)^{N/2} |\Lambda_1|^{1/2} \exp \left\{ \frac{1}{2} (\mathbf{t}_{R,2}^{tr} + \mathbf{t}_{R,3}^{tr}) \Lambda_1 (\mathbf{t}_{R,2} + \mathbf{t}_{R,3}) \right\}, \end{aligned}$$

after evaluating the integral. We finally obtain (19). \square

Remark 12. *If the initial condition is unknown, our approach allows the incorporation of its random modeling and the corresponding marginalization step.*

Remark 13. *The marginal likelihood (19) is actually valid for any linear evolution model given by (15). In fact, this framework can be extended to time dependent linear PDEs and the marginalization procedure is independent from the dimension of the PDE.*

5 A Bayesian inference for thermal diffusivity

In this section, we implement our Bayesian approach to infer the thermal diffusivity θ , an unknown parameter that appears in the heat equation and measures the rapidity of the heat propagation through a material (dos Santos et al., 2005).

Synthetic data are used to simulate as close as possible the experimental measurements of heat conduction properties by Lanzarone et al. (2014) that, although unavailable for public use, have inspired the present work. Those authors considered the thermal properties of a polymethyl methacrylate specimen when submitted to heating and cooling cycles in a range of temperatures between 25 and 90 °C, measured by thermocouples in 5 inner, equispaced points and 2 outer ones. In particular, comparison of our Figure 1 with the cooling phase of Experiment B in Figure 4 of Lanzarone et al. (2014) presents a similar behavior.

Consider the heat equation (one-dimensional diffusion equation for $T(x, t)$):

$$\begin{cases} \partial_t T - \partial_x (\theta(x) \partial_x T) = 0, & x \in (x_L, x_R), 0 < t \leq t_N < \infty \\ T(0, t) = T_L(t), & t \in [0, t_N] \\ T(1, t) = T_R(t), & t \in [0, t_N] \\ T(x, 0) = g(x), & x \in (x_L, x_R). \end{cases} \quad (20)$$

We want to infer the thermal diffusivity, $\theta(x)$, using a Bayesian approach when the temperature is measured at $I + 1$ locations, $x_0 = x_L, x_1, x_2, \dots, x_{I-1}, x_I = x_R$, at each of the N times, t_1, t_2, \dots, t_N . Clearly, this problem is a special case of (1) where $L_\theta = -\partial_x(\theta(x)\partial_x T)$ and $\theta(x) > 0$. We can therefore immediately obtain the non-normalized posterior distribution of θ using the marginal likelihood (19).

The prior distributions for θ can be specified in different ways. In this section we will consider two cases, when θ is a lognormal random variable and when θ depends on the space variable x and is modeled by means of a lognormal random field. We focus on the second case in Subsection 5.3. We start by discussing the case where the thermal diffusivity prior is independent of x .

If we consider a lognormal prior $\log \theta \sim \mathcal{N}(\nu, \tau)$, where $\nu \in \mathbb{R}$ and $\tau > 0$, then the non-normalized posterior distribution of θ is given by

$$\rho_{\nu, \tau}(\theta | \mathbf{Y}_1, \dots, \mathbf{Y}_N) \propto \frac{1}{\sqrt{2\pi}\theta\tau} \exp\left(-\frac{(\log \theta - \nu)^2}{2\tau^2}\right) \rho(\mathbf{Y}_1, \dots, \mathbf{Y}_N | \theta). \quad (21)$$

The posterior distribution of θ can be approximated by Laplace’s method (Ghosh et al. (2006), Chapter 4) to obtain a Gaussian posterior

$$\rho_{\nu, \tau}(\theta | \mathbf{Y}_1, \dots, \mathbf{Y}_N) \approx \frac{1}{\sqrt{2\pi|H(\hat{\theta})|}} \exp\left\{-\frac{1}{2}(\theta - \hat{\theta})^T H(\hat{\theta})^{-1}(\theta - \hat{\theta})\right\}$$

where $\hat{\theta}$ is the maximum a posteriori (MAP) probability estimate of θ and $H(\hat{\theta})$ is the inverse Hessian matrix of the negative log posterior evaluated at $\hat{\theta}$.

To assess the behavior of our method, we introduce a synthetic dataset generated with constant θ . Let us assume, without loss of generality, that the interval time $[0, t_N]$ is equal to $[0, 1]$, $x_L = 0$ and $x_R = 1$.

Dataset A

In order to generate data, we solve the initial-boundary value problem for the heat equation with Robin boundary conditions:

$$\begin{aligned} \partial_x T(x_L, t) &= \frac{h}{\kappa} (T(x_L, t) - T_{out}), \quad t \in [0, 1], \\ \partial_x T(x_R, t) &= \frac{h}{\kappa} (T_{out} - T(x_R, t)), \quad t \in [0, 1], \end{aligned}$$

and the initial condition $T(x, 0) = T_0$, $x \in (0, 1)$, where $\theta(x) = 1 \times 10^{-7} \text{ m}^2/\text{s}$, h is the convective heat transfer coefficient, κ denotes the thermal conductivity, $\frac{h}{\kappa} = 1 (1/m)$, $T_{out} = 20^\circ\text{C}$ and $T_0 = 100^\circ\text{C}$ (see Figure 1).

A synthetic dataset (hereafter named dataset A) is generated, with a measurement standard error noise of $\sigma_d = 0.56$.

Before presenting the implementation of our novel technique, we will show how the Bayesian method works, using the joint likelihood (7), under the very restrictive assumption that the temperature values at the boundaries are exactly known.

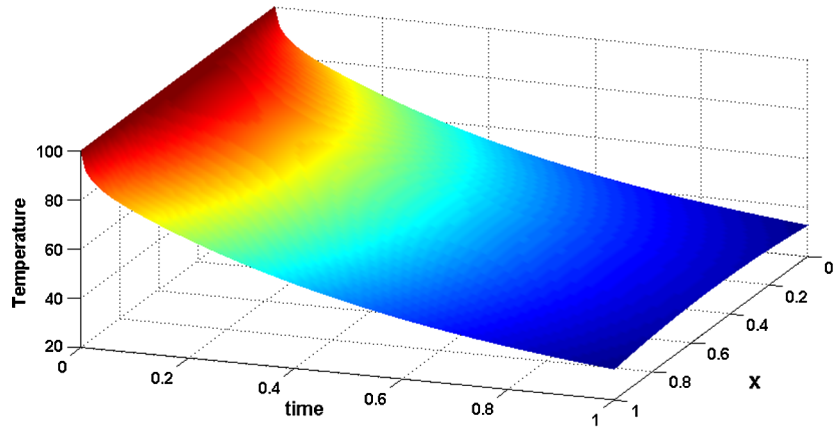


Figure 1: Exact solution of the initial-boundary value problem for the heat equation, $\theta = 1 \times 10^{-7} \text{ m}^2/\text{s}$.

5.1 Example 1

Suppose that the thermal diffusivity, θ , is a random variable with a lognormal prior, $\log \theta \sim \mathcal{N}(\nu, \tau)$. In this case, the non-normalized posterior density for θ is given by

$$\rho_{\nu, \tau}(\theta | \mathbf{Y}_1, \dots, \mathbf{Y}_N) \propto \frac{1}{\sqrt{2\pi\theta\tau}} \exp\left(-\frac{(\log \theta - \nu)^2}{2\tau^2}\right) \exp\left(-\frac{1}{2\sigma^2} \sum_{n=1}^N \|\mathbf{R}_{t_n}\|_{\ell^2}^2\right),$$

where \mathbf{R}_{t_n} is used here because the boundary data are known exactly.

Given that θ is a lognormal random variable with $\nu = \tau = 0.1$, the resulting posterior will depend on σ and the number of observations N that are used to compute the log-likelihood. Figure 2 shows the behavior of the log-likelihood and the log-posterior for θ using different values for σ and N .

We then use the Laplace approximation to derive the Gaussian posterior approximated density for θ . The prior and posterior densities for θ are presented in Figure 3, where it can be appreciated that we obtained a Gaussian posterior, with mean 1.0025 and standard deviation 0.0044, which is concentrated around the true value of the parameter, θ , despite having a very broad prior. We are now in the position to extend our implementation to embrace the case where the temperature values at the boundaries are unknown parameters as well.

5.2 Example 2

In this example, we consider again θ as a random variable with a lognormal prior, $\log \theta \sim \mathcal{N}(\nu, \tau)$. Unlike Example 1, we assume noisy boundary measurements and a Gaussian prior distribution for the boundary parameters as in (17). Therefore, the non-

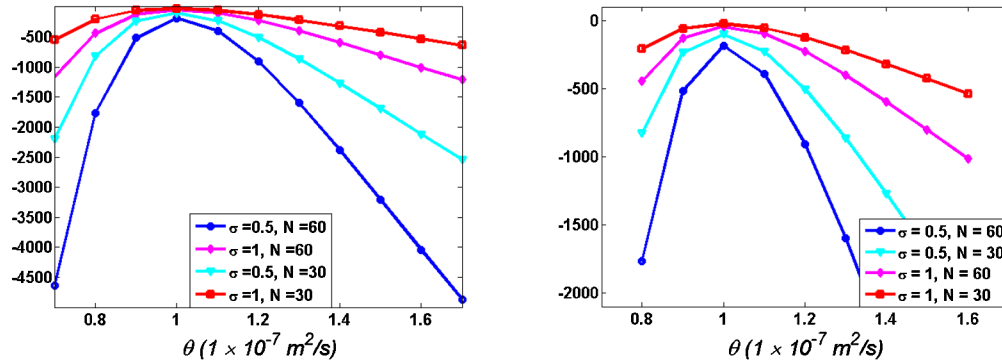


Figure 2: Example 1: Comparison between log-likelihoods (on the left) and log-posteriors (on the right) for θ using different numbers of observations, N , and different values of σ .

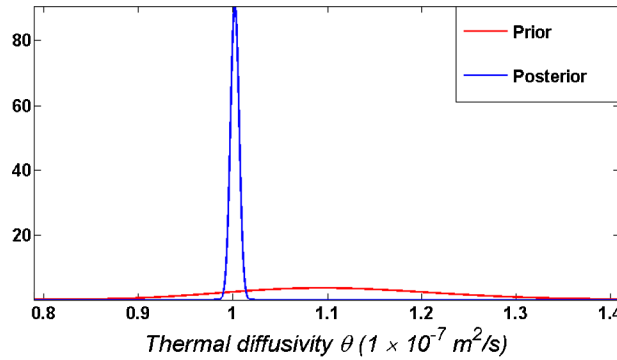


Figure 3: Example 1: Lognormal prior and approximated Gaussian posterior densities for θ , where $\sigma_p = \sigma = 0.5$ and $N = 60$.

normalized posterior density for θ is given by

$$\rho_{\nu,\tau}(\theta|\mathbf{Y}_1, \dots, \mathbf{Y}_N) \propto \frac{1}{\sqrt{2\pi\theta\tau}} \exp\left(-\frac{(\log \theta - \nu)^2}{2\tau^2}\right) \rho(\mathbf{Y}_1, \dots, \mathbf{Y}_N|\theta),$$

where $\rho(\mathbf{Y}_1, \dots, \mathbf{Y}_N|\theta)$ is the marginal likelihood of θ defined in Theorem 11.

Remark 14. Since $\theta(x)$ is supposed to be constant, we can obtain equation (15) alternatively by solving the heat equation using finite differences (see Appendix C of the Supplementary Material).

Numerical results are now presented using the synthetic dataset A and assuming that θ is a lognormal random variable with $\nu = \tau = 0.1$. Figure 4 shows the behavior of the log-likelihood and the log-posterior for θ using different values of N and σ . Clearly, the accuracy of the estimated θ depends on the size of the dataset, N , and the reliability of measurement devices, σ .

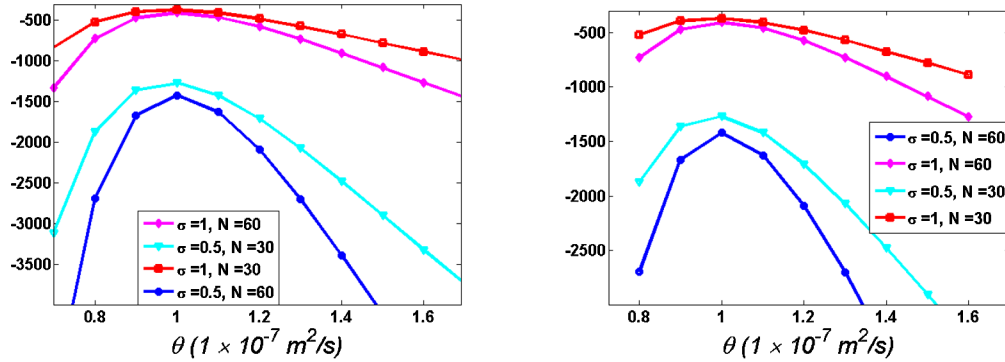


Figure 4: Example 2: Comparison between log-likelihoods (on the left) and log-posteriors (on the right) for θ using different numbers of observations, N , and different values of σ .

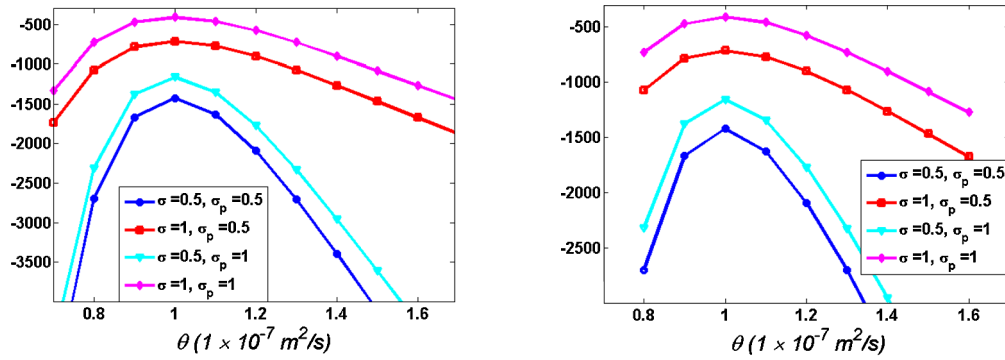


Figure 5: Example 2: Comparison between log-likelihoods (on the left) and log-posteriors (on the right) for θ using different values of σ and σ_p , with $N = 60$.

Figure 5 shows the relationship between the prior distribution of the boundary conditions and their measurements. Although we notice different behaviors of the log-likelihood and the log-posterior, these functions exhibit the same argument of the maximum which is close to the true value of θ .

Again, the Laplace approximation is used to derive the Gaussian posterior approximated density for θ . The prior and posterior densities for θ are presented in Figure 6 in which the Gaussian posterior, with mean 0.9955 and standard deviation 0.0047, is concentrated around the true value of θ unlike the very broad prior.

Convergence of MAP estimates

When using numerical methods to approximate the dynamic process, it is important to control the discretization error because it produces a bias error in the statistical

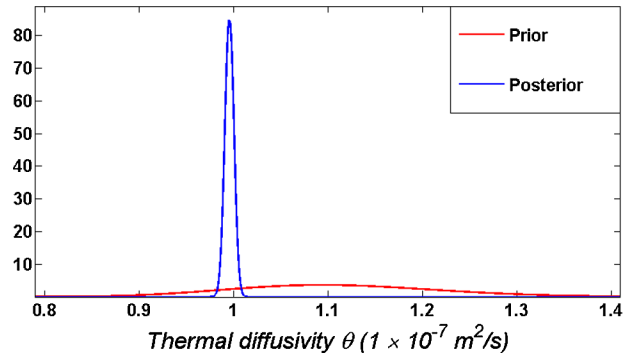


Figure 6: Example 2: Lognormal prior and approximated Gaussian posterior densities for θ where $\sigma_p = \sigma = 0.5$ and $N = 60$.

inference. Many methods are developed to assess the impact of the discretization error when PDEs are used in a statistical framework. In particular, very recently, Conrad et al. (2015) have introduced probability measures over the numerical solutions by randomizing the deterministic solvers.

Here, we show that MAP estimates have the same convergence rate as the numerical solver used to obtain the marginal likelihood (19). For this purpose, we present the results from basic convergence tests with respect to discretization space size, Δx , and discretization time step, Δt , to ensure that the discretization error is negligible in comparison with the statistical error.

The numerical solver is based on finite element method with piecewise linear functions to approximate the solution in space and backward Euler discretization in time (see Section 3). Equivalently, we can use centered difference in space and backward difference in time (see Appendix C of the Supplementary Material). Therefore, the convergence rate of our solver is quadratic in space and linear in time. MAP estimates are obtained by means of the MATLAB function `fmincon`, which is suitable to minimize the negative log-posterior with a prescribed tolerance equal to 1×10^{-16} .

Figures 7 and 8 show that the MAP estimates of θ converge quadratically with Δx and linearly with Δt , which is consistent with the chosen solver. The above criteria aim to check that the discretization error is smaller than the statistical error, and they apply when the thermal diffusivity is modeled as a random field.

Information divergence and expected information gain

In the Bayesian setting that we adopted to infer the thermal diffusivity, θ , the utility of the performed experiment, given an experimental setup ξ , can be conveniently measured by the so-called information divergence (or discrimination information as Kullback (1987) called it), which is here defined as the Kullback–Leibler divergence (Kullback and Leibler (1951)) between the prior density function $p(\theta)$ and the posterior

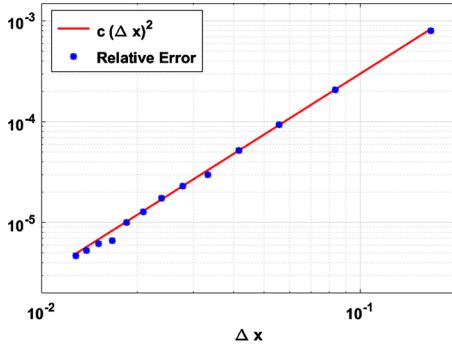


Figure 7: Example 2: Convergence of MAP estimates of θ with respect to Δx .

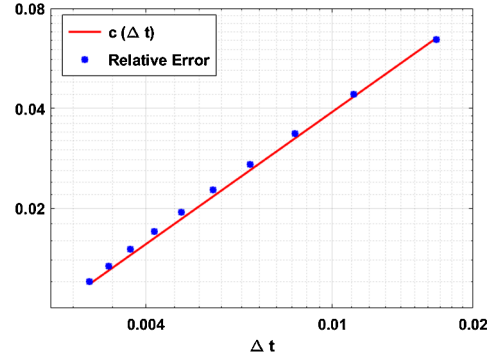


Figure 8: Example 2: Convergence of MAP estimates of θ with respect to Δt .

density function of θ , $\rho(\theta|\mathbf{Y}_1, \dots, \mathbf{Y}_N, \xi)$:

$$D_{KL}(\mathbf{Y}_1, \dots, \mathbf{Y}_N, \xi) := \int_{\Theta} \log \left(\frac{\rho(\theta|\mathbf{Y}_1, \dots, \mathbf{Y}_N, \xi)}{p(\theta)} \right) \rho(\theta|\mathbf{Y}_1, \dots, \mathbf{Y}_N, \xi) d\theta. \quad (22)$$

The quantity in (22) is always non-negative; it is equal to zero when the prior and the posterior coincide; it provides a quantification of the relative discrimination between the prior and the posterior; and it depends on the observations $\mathbf{Y}_1, \dots, \mathbf{Y}_N$. Therefore, given the synthetic dataset, A , we may introduce different experimental setups of interest by varying the interval time during which the temperature is measured. By choosing some specific thermocouples, we may evaluate the information divergence for any experimental setup. Moreover, under the same generating process used for the dataset A , we may obtain as many synthetic datasets as needed to explore the properties of the proposed simulated experiment. The utility of such computer-based experiments can be adequately summarized by the so-called expected information gain (Long et al. (2013)), which is defined as the marginalization of D_{KL} over all possible simulated data:

$$I(\xi) := \int_{\mathcal{Y}} \int_{\Theta} \log \left(\frac{\rho(\theta|\mathbf{Y}_1, \dots, \mathbf{Y}_N, \xi)}{p(\theta)} \right) \rho(\theta|\mathbf{Y}_1, \dots, \mathbf{Y}_N, \xi) d\theta \rho(\{\mathbf{Y}_i\}_{i=1}^N | \xi) d(\{\mathbf{Y}_i\}_{i=1}^N). \quad (23)$$

This quantity (23) provides a criterion to determine which features of the setup, ξ , are, on average, most informative when inferring θ . A larger value of $I(\xi)$ when, say, $\xi \in A$, suggests that, given the proposed statistical model, the inference on the unknown parameter will be more efficient, on average, when the features of the designed experiment take value in the set A .

Let us label as TC1, \dots , TC7 the thermocouples from the left boundary to the right boundary, respectively.

The numerical estimations of the information divergence for the synthetic dataset A and of the expected information gain, by using (21) to compute the approximated

posterior in Example 1, are shown in Figures 9, 10 and 11, which refer to the following three experimental setups (es's):

- es1) ξ consists of three non-overlapping time intervals, with the same length, which cover the entire observational period $[0, 1]$;
- es2) ξ consists of the five inner thermocouples;
- es3) ξ is the combination of the two previous experimental setups, es1 and es2.

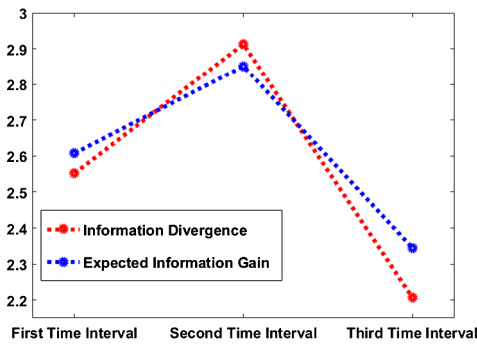


Figure 9: Example 2: The expected information gain compared with the information divergence for dataset A, for the three time intervals experimental setup (es1).

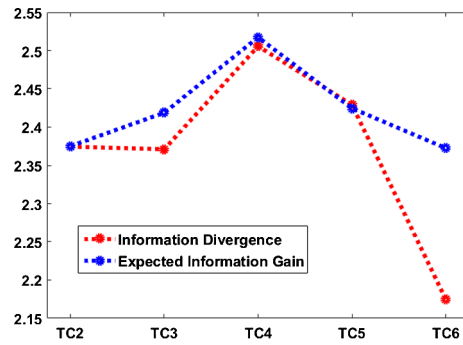


Figure 10: Example 2: The expected information gain compared with the information divergence for dataset A, for the five inner thermocouples experimental setup (es2).

From the values in Figure 9, which depicts the results from an experimental setup in which the temperature measurements are collected at different time intervals, we may conclude, by virtue of the interpretation of the expected information gain, that the second time interval is the most informative time interval from which to draw inferences on the thermal diffusivity, whereas the last time interval is the least informative one.

Figure 10 summarizes how the expected information gain behaves for the five inner thermocouples experimental setup (es2). Given the synthetic dataset A, the sixth thermocouple (TC6) is the one where the information divergence takes the smallest value. However, when we look at the expected information gain, we may appreciate the nearly symmetric informative content of the thermocouples with respect to the central thermocouple (TC4) and how the expected gain about the thermal diffusivity becomes larger near the central thermocouple.

Finally, we look for the best combination of the two previous experimental setups, and the corresponding results are displayed in Figure 11. We observe that the highest expected information gain is attained at the middle thermocouple (TC4) by using the information collected during the second time interval. Any indication provided by the

numerical estimation of the expected information gain is very valuable to an experimentalist, since it suggests the most relevant features to be considered to build up an efficient experiment to infer the unknown parameters of the assumed statistical model.

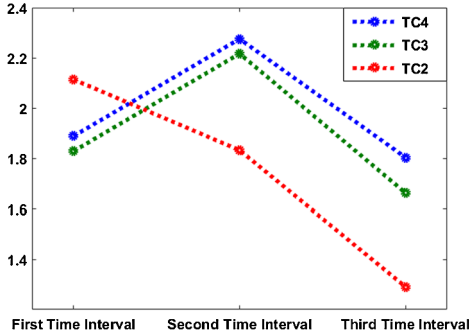


Figure 11: Example 2: The expected information gain for the combination (es3) of the three time intervals and the five inner thermocouples experimental setups.

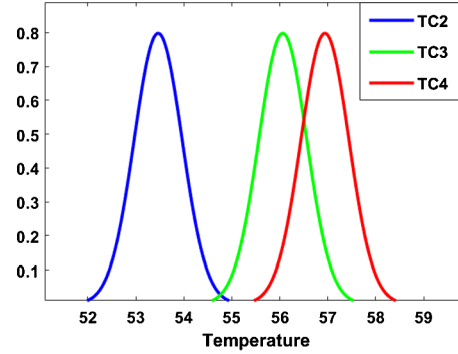


Figure 12: Example 2: The predictive posterior densities of the observable temperatures for the thermocouples TC2, TC3, TC4 at time $t = 0.52$.

Predictive posterior distribution

In this section, we examine the possibility of predicting the observable temperature at future time intervals after estimating the thermal diffusivity, θ . More specifically, assume we have inferred θ using temperature measurements up to time t_n . Then, we want to predict the temperature in the next time step, t_{n+1} . Given our Bayesian model, it is necessary to assume the knowledge of the boundary temperature at time t_{n+1} . A typical situation could be given by an experiment in which there is interest in temperature values at inner points for different boundary values.

The predictive posterior distribution, $\rho(\mathbf{Y}_{n+1} | \{\mathbf{Y}_{\mathbf{k}}\}_{k=1}^n, T_{L,n+1}, T_{R,n+1})$, is given by

$$\int_{\Theta} \rho(\mathbf{Y}_{n+1} | \{\mathbf{Y}_{\mathbf{k}}\}_{k=1}^n, T_{L,n+1}, T_{R,n+1}, \theta) \rho(\theta | \{\mathbf{Y}_{\mathbf{k}}\}_{k=1}^n) d\theta, \quad (24)$$

and it is estimated by averaging

$$\frac{1}{M} \sum_{i=1}^M \rho(\mathbf{Y}_{n+1} | \{\mathbf{Y}_{\mathbf{k}}\}_{k=1}^n, T_{L,n+1}, T_{R,n+1}, \theta_i),$$

where the θ_i 's are sampled from the posterior distribution of θ .

Figure 12 shows the one-step-ahead predictive posterior densities at three different inner thermocouples based on the observations until time $t = 0.5$, when the observed temperature at thermocouples TC2, TC3 and TC4 were 53.98, 55.53 and 57.84 °C respectively.

We emphasize that this methodology allows us to obtain the k-step ahead predictive posterior density for any inner thermocouple, assuming boundary conditions subject to uncertainty that are adequate for the experiment.

5.3 Example 3

In this example, we consider the case where the thermal diffusivity depends on the space variable, x . The finite element method used to solve the heat equation under such an assumption was presented in Section 3.

Prior distribution of $\theta(x)$

Assume that the prior distribution of $\theta(x)$ is a lognormal random field with a squared exponential (SE) covariance function. Then, the prior distribution of $\log \theta(x)$ can be expressed using the joint multivariate Gaussian distribution:

$$(\log(\theta(x_1)), \dots, \log(\theta(x_s))) \sim \mathcal{N}_s(\boldsymbol{\mu}, K), \tag{25}$$

where $\boldsymbol{\mu} = (\mu, \mu, \dots, \mu)^{tr}$, $K_{ij} = Cov(\log(\theta(x_i)), \log(\theta(x_j))) = \eta^2 \exp(-\frac{|x_i - x_j|^2}{2\ell})$, $i, j = 1, \dots, s$, η is the magnitude, and ℓ denotes the length scale.

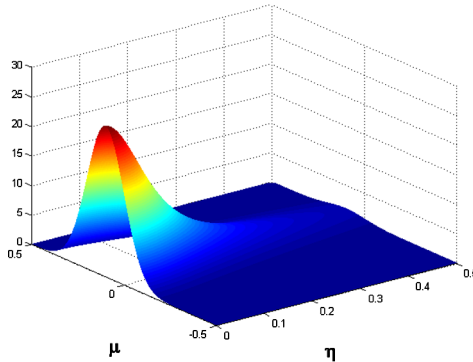


Figure 13: Example 3: Joint prior density for the hyperparameters μ and η , with $\mu \sim \mathcal{N}(0.1, 0.1)$ and $\eta \sim \text{half-Cauchy}(0.1)$.

We assume the following priors for the hyperparameters μ, η and ℓ (the prior density of μ and η is displayed in Figure 13):

$$\mu \sim \mathcal{N}(0.1, 0.1), \quad \eta \sim \text{half-Cauchy}(0.1), \quad \ell \sim U(0.5, 5).$$

In this example, we choose a Gaussian prior for μ and uninformative uniform prior for ℓ . The half-Cauchy prior for η was chosen because it is a practical prior for scale parameters in hierarchical models (Polson and Scott, 2012) (Gelman, 2006).

Joint posterior distribution of the hyperparameters μ, η, ℓ

Given $\boldsymbol{\theta} := (\theta(x_1), \dots, \theta(x_s))^{tr}$, let us consider the joint posterior density of the hyperparameters (μ, η, ℓ) that characterize the distribution of $\log \theta(x)$

$$\rho(\mu, \eta, \ell | \mathbf{Y}_1, \dots, \mathbf{Y}_N) \propto \rho(\mu, \eta, \ell) \int_{\Theta} \rho(\boldsymbol{\theta} | \mu, \eta, \ell) \rho(\mathbf{Y}_1, \dots, \mathbf{Y}_N | \boldsymbol{\theta}) d\boldsymbol{\theta}.$$

Let us introduce the auxiliary variable $\mathbf{z} = (z_1, \dots, z_s) \sim \mathcal{N}_s(\mathbf{0}, C = \frac{1}{\eta^2} K)$ and consider the change of variables transformation: $\log(\theta_i) = \mu + \eta z_i$ where $\theta_i := \theta(x_i)$, $z_i := z(x_i)$, $i = 1, \dots, s$. Then, the prior density of $\boldsymbol{\theta}$ is given by

$$\begin{aligned} \rho(\boldsymbol{\theta} | \mu, \eta, \ell) &= \frac{(\eta^2 2\pi)^{-\frac{s}{2}} |C|^{-\frac{1}{2}}}{\theta_1 \theta_2 \dots \theta_s} \exp\left(-\frac{(\log \boldsymbol{\theta} - \boldsymbol{\mu})^{tr} C (\log \boldsymbol{\theta} - \boldsymbol{\mu})}{2\eta^2}\right) \\ &= \frac{(2\pi)^{-\frac{s}{2}} |C|^{-\frac{1}{2}}}{\eta^s e^{s\mu + \eta(z_1 + \dots + z_s)}} \exp\left(-\frac{1}{2} \mathbf{z}^{tr} C^{-1} \mathbf{z}\right) \\ &= \frac{\rho(\mathbf{z} | \ell)}{\eta^s e^{s\mu + \eta(z_1 + \dots + z_s)}}. \end{aligned}$$

The posterior density of the hyperparameters can be therefore written as

$$\rho(\mu, \eta, \ell | \mathbf{Y}_1, \dots, \mathbf{Y}_N) \propto \rho(\mu, \eta, \ell) \int_{\mathbf{Z}} \frac{\rho(\mathbf{z} | \ell)}{\eta^s e^{s\mu + \eta(z_1 + \dots + z_s)}} |J| \rho(\mathbf{Y}_1, \dots, \mathbf{Y}_N | \mu, \eta, \mathbf{z}) d\mathbf{z},$$

where J is the Jacobian matrix of the transformation.

By considering ℓ as a nuisance parameter, we obtain

$$\rho(\mu, \eta | \mathbf{Y}_1, \dots, \mathbf{Y}_N) \propto \rho(\mu, \eta) \int_{\ell} \rho(\ell) \int_{\mathbf{Z}} \rho(\mathbf{z} | \ell) \rho(\mathbf{Y}_1, \dots, \mathbf{Y}_N | \mu, \eta, \mathbf{z}) d\mathbf{z} d\ell \quad (26)$$

after ℓ is marginalized.

To evaluate the posterior distribution of the hyperparameters, we need to compute the $s + 1$ dimensional integral in formula (26). Alternatively, Monte Carlo method can be used to approximate these integrals. First, we sample ℓ from its prior distribution, $\rho(\ell)$. Then, given ℓ we can sample \mathbf{z} and evaluate the joint likelihood function, $\rho(\mathbf{Y}_1, \dots, \mathbf{Y}_N | \mu, \eta, \mathbf{z})$, for any pair (μ, η) . Therefore, we approximate the non-normalized posterior distribution using a double sum as follows:

$$\begin{aligned} \int_{\ell} \rho(\ell) \int_{\mathbf{Z}} \rho(\mathbf{z} | \ell) \rho(\mathbf{Y}_1, \dots, \mathbf{Y}_N | \mu, \eta, \mathbf{z}) d\mathbf{z} d\ell &\approx \frac{1}{M_{\ell}} \sum_{i=1}^{M_{\ell}} \int_{\mathbf{Z}} \rho(\mathbf{z} | \ell_i) \rho(\mathbf{Y}_1, \dots, \mathbf{Y}_N | \mu, \eta, \mathbf{z}) d\mathbf{z} \\ &\approx \frac{1}{M_{\ell}} \frac{1}{M_z} \sum_{i=1}^{M_{\ell}} \sum_{j=1}^{M_z} \rho(\mathbf{Y}_1, \dots, \mathbf{Y}_N | \mu, \eta, \mathbf{z}_j), \end{aligned}$$

where $\mathbf{z}_j \sim \rho(\mathbf{z} | \ell_i)$.

Figure 14 shows that the non-normalized posterior of the hyperparameters μ and η has a unique mode at $(-0.05, 0.025)$. We use then Laplace's method to obtain a Gaussian posterior, using the synthetic dataset A, as shown in Figure 15.

A new dataset is now introduced to test our method when θ depends on x .

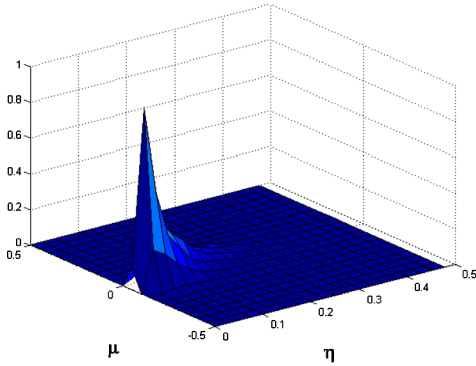


Figure 14: Example 3: Non-normalized joint posterior density of the hyperparameters μ and η .

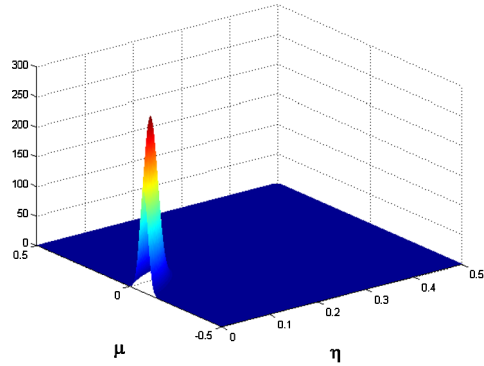


Figure 15: Example 3: Laplace's approximation of the posterior density of the hyperparameters μ and η .

Dataset B

To analyze the performance of our inferential technique in the case where the thermal diffusivity parameter depends on the space variable, x , we consider another synthetic dataset (hereafter named dataset B) that is generated similarly to the dataset A, except for the fact that $\theta(x)$ is sampled randomly from the new prior (25) where $\mu = 0, \eta = 0.1$ and $\ell = 5$.

Again, we approximate the posterior distribution of the hyperparameters μ and η using Laplace's approximation given the following priors for the hyperparameters μ, η and ℓ (the prior density of μ and η is displayed in Figure 16):

$$\mu \sim \mathcal{N}(0, 0.25), \quad \eta \sim \text{half-Cauchy}(0.5), \quad \ell \sim U(4, 6),$$

where we assume broad priors for μ and η with a more informative uniform prior for ℓ .

From Figure 17, we find that the maximum a posteriori probability (MAP) estimate is $(0.05, 0.025)$ and Laplace's approximation can be used. By comparing the prior and posterior densities for μ and η in Figures 16 and 18, we can say that the experiment is informative since the posterior concentrates around $(0.05, 0.025)$ which is close to the true value.

6 Conclusion

In this work, we developed a general Bayesian approach for one-dimensional linear parabolic partial differential equations with noisy boundary conditions. First, we derived the joint likelihood of the thermal diffusivity θ and the boundary parameters. Second, we approximated the solution of the forward problem, by showing that such solution can be written as a linear function of the boundary conditions. After that, we marginalized out the boundary parameters, under the assumptions that they are

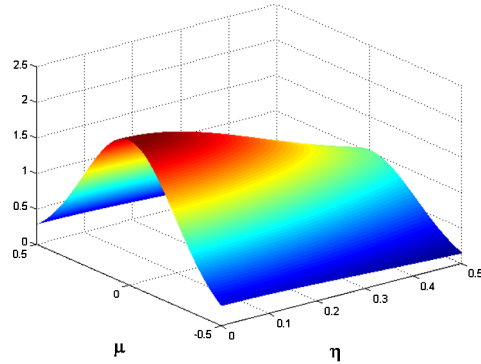


Figure 16: Example 3: Joint prior density for the hyperparameters μ and η , with $\mu \sim \mathcal{N}(0, 0.25)$ and $\eta \sim \text{half-Cauchy}(0.5)$.

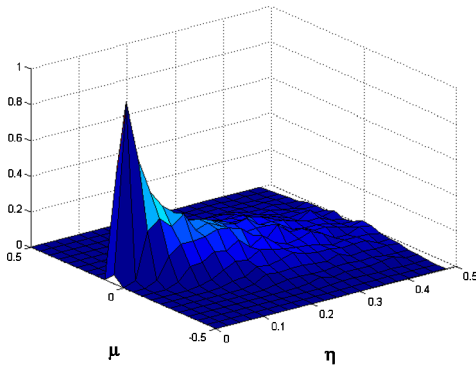


Figure 17: Example 3: Non-normalized joint posterior density of the hyperparameters μ and η .

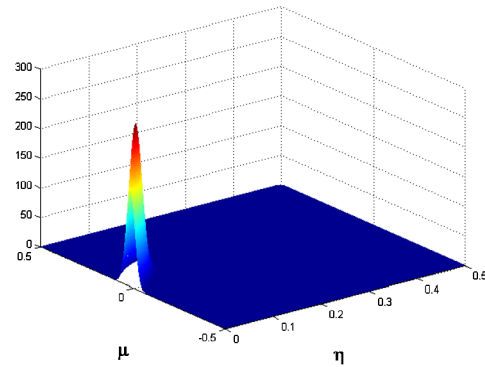


Figure 18: Example 3: Laplace's approximation for the posterior density of the hyperparameters μ and η .

well approximated by piecewise linear functions and that they are independent Gaussian random vectors. This approach can be generalized to any well-posed linear partial differential equation.

On the implementation side, we computed the log-posterior of the thermal diffusivity in different cases. Besides, we used the Laplace approximation to obtain a Gaussian posterior. In the first example, we used directly the joint likelihood of the thermal diffusivity θ and the boundary parameters, assuming that the boundary conditions were known. In the second example, we used the marginalized likelihood of θ , assuming that θ is a lognormal random variable and, as in the previous example, we obtained an approximated Gaussian posterior distribution, showing that the unknown value of the thermal diffusivity is recovered almost exactly. Moreover, we explored two important advantages of using the Bayesian approach, by providing the

estimation of the expected information gain for different experimental setups and the predictive posterior distribution of the temperature. We noticed that the temperature measurements from the middle thermocouple at the second time interval are, in general, the most informative measurements. Finally, assuming that θ is a lognormal random field with squared exponential covariance function, we evaluated the joint posterior distribution for the covariance hyperparameters by applying hierarchical Bayesian techniques.

Supplementary Material

Supplementary material for “A hierarchical Bayesian setting for an inverse problem in linear parabolic PDEs with noisy boundary conditions” (DOI: [10.1214/16-BA1007SUPP.pdf](https://doi.org/10.1214/16-BA1007SUPP.pdf)). Supplementary material includes proofs of Theorem 7, Theorem 8 and Remark 14.

References

- Bär, M., Hegger, R., and Kantz, H. (1999). “Fitting partial differential equations to space-time dynamics.” *Physical Review E*, 59(1): 337–342. [408](#)
- Charrier, J. (2012). “Strong and weak error estimates for elliptic partial differential equations with random coefficients.” *SIAM Journal on Numerical Analysis*, 50(1): 216–246. [MR2888311](#). doi: <http://dx.doi.org/10.1137/100800531>. [411](#)
- Conrad, P. R., Girolami, M., Särkkä, S., Stuart, A., and Zygalakis, K. (2015). “Probability measures for numerical solutions of differential equations.” [arXiv:1506.04592](#). [423](#)
- dos Santos, W. N., Mummery, P., and Wallwork, A. (2005). “Thermal diffusivity of polymers by the laser flash technique.” *Polymer Testing*, 24(5): 628–634. [418](#)
- Evans, L. C. (1998). *Partial Differential Equations*. American Mathematical Society. [MR1625845](#). [410](#)
- Fudym, O., Orlande, H., Bamford, M., and Batsale, J. (2008). “Bayesian approach for thermal diffusivity mapping from infrared images with spatially random heat pulse heating.” *Journal of Physics: Conference Series*, 135(1): 012042. [409](#)
- Gelman, A. (2006). “Prior distributions for variance parameters in hierarchical models (comment on article by Browne and Draper).” *Bayesian Analysis*, 1(3): 515–534. [MR2221284](#). [427](#)
- Ghosh, J. K., Delampady, M., and Samanta, T. (2006). *An Introduction to Bayesian Analysis*. Springer. [MR2247439](#). [408](#), [419](#)
- Johnson, C. (1987). *Numerical Solution of Partial Differential Equations by the Finite Element Method*. Cambridge University Press. [MR0925005](#). [414](#), [415](#)
- Kaipio, J. P. and Fox, C. (2011). “The Bayesian framework for inverse problems in heat transfer.” *Heat Transfer Engineering*, 32(9): 718–753. [408](#), [409](#)

- Kullback, S. (1987). “The Kullback–Leibler distance.” *The American Statistician. Letters to the Editor*, 41(4): 340–341. 423
- Kullback, S. and Leibler, R. (1951). “On information and sufficiency.” *The Annals of Mathematical Statistics*, 22(1): 79–86. MR0039968. 423
- Lanzarone, E., Pasquali, S., Mussi, V., and Ruggeri, F. (2014). “Bayesian estimation of thermal conductivity and temperature profile in a homogeneous mass.” *Numerical Heat Transfer, Part B: Fundamentals*, 66(5): 397–421. 409, 418
- Long, Q., Scavino, M., Tempone, R., and Wang, S. (2013). “Fast estimation of expected information gains for Bayesian experimental designs based on Laplace approximations.” *Computer Methods in Applied Mechanics and Engineering*, 259(1): 24–39. MR3063259. doi: <http://dx.doi.org/10.1016/j.cma.2013.02.017>. 424
- Massard, H., Fudym, O., Orlande, H., and Batsale, J. (2010). “Nodal predictive error model and Bayesian approach for thermal diffusivity and heat source mapping.” *Comptes Rendus Mécanique*, 338(7–8): 434–449. 409
- Müller, T. G. and Timmer, J. (2002). “Fitting parameters in partial differential equations from partially observed noisy data.” *Physica D: Nonlinear Phenomena*, 171(1): 1–7. MR1930816. doi: [http://dx.doi.org/10.1016/S0167-2789\(02\)00546-8](http://dx.doi.org/10.1016/S0167-2789(02)00546-8). 408
- Polson, N. G. and Scott, J. G. (2012). “On the half-Cauchy prior for a global scale parameter.” *Bayesian Analysis*, 7(4): 887–902. MR3000018. doi: <http://dx.doi.org/10.1214/12-BA730>. 427
- Ramsay, J. O., Hooker, G., Campbell, D., and Cao, J. (2007). “Parameter estimation for differential equations: a generalized smoothing approach.” *Journal of the Royal Statistical Society, Series B*, 69(5): 741–796. MR2368570. doi: <http://dx.doi.org/10.1111/j.1467-9868.2007.00610.x>. 408
- Rasmussen, C. E. and Williams, C. K. (2006). *Gaussian Processes for Machine Learning*. the MIT Press. MR2514435. 409
- Ruggeri, F., Sawlan, Z., Scavino, M., and Tempone, R. (2016). Supplementary material for “A hierarchical Bayesian setting for an inverse problem in linear parabolic PDEs with noisy boundary conditions” *Bayesian Analysis*. doi: <http://dx.doi.org/10.1214/16-BA1007SUPP>. 415
- Samarskii, A. A. and Vabishchevich, P. N. (2007). *Numerical Methods for Solving Inverse problems of Mathematical Physics*. Walter de Gruyter. MR2381619. doi: <http://dx.doi.org/10.1515/9783110205794>. 408
- Wang, J. and Zabaras, N. (2004). “A Bayesian inference approach to the inverse heat conduction problem.” *International Journal of Heat and Mass Transfer*, 47(17–18): 3927–3941. 409
- Wang, J. and Zabaras, N. (2005). “Hierarchical Bayesian models for inverse problems in heat conduction.” *Inverse Problems*, 21(1): 183–206. MR2146171. doi: <http://dx.doi.org/10.1088/0266-5611/21/1/012>. 409

Xun, X., Cao, J., Mallick, B., Maity, A., and Carroll, R. J. (2013). “Parameter estimation of partial differential equation models.” *Journal of the American Statistical Association*, 108(503): 1009–1020. MR3174680. doi: <http://dx.doi.org/10.1080/01621459.2013.794730>. 408, 409

Acknowledgments

Part of this work was carried out while F. Ruggeri and M. Scavino were Visiting Professors at KAUST. Z. Sawlan, M. Scavino and R. Tempone are members of the KAUST SRI Center for Uncertainty Quantification in Computational Science and Engineering.